Evolution of dispersal under variable connectivity

Petteri Karisto* & Éva Kisdi†

Department of Mathematics and Statistics
University of Helsinki, Finland

This article has been published in the Journal of Theoretical Biology:
http://dx.doi.org/10.1016/j.jtbi.2016.11.007

Please cite as: Karisto P. and Kisdi E. 2017. Evolution of dispersal under variable connectivity. J. theor. Biol. 419: 52–65.

Keywords: adaptive dynamics, dispersal polymorphism, evolutionary branching, kin competition, patch connectivity

Mathematics Subject Classification: 92D15, 92D25, 92D40

Abstract. The pattern of connectivity between local populations or between microsites supporting individuals within a population is a poorly understood factor affecting the evolution of dispersal. We modify the well-known Hamilton–May model of dispersal evolution to allow for variable connectivity between microsites. For simplicity, we assume that the microsites are either solitary, i.e., weakly connected through costly dispersal, or part of a well-connected cluster of sites with low-cost dispersal within the cluster. We use adaptive dynamics to investigate the evolution of dispersal, obtaining analytic results for monomorphic evolution and numerical results for the co-evolution of two dispersal strategies. A monomorphic population always evolves to a unique singular dispersal strategy, which may be an evolutionarily stable strategy or an evolutionary branching point. Evolutionary branching happens if the contrast between connectivities is sufficiently high and the solitary microsites are common. The dimorphic evolutionary singularity, when it exists, is always evolutionarily and convergence stable. The model exhibits both protected and unprotected dimorphisms of dispersal strategies, but the dimorphic singularity is always protected. Contrasting connectivities can thus maintain dispersal polymorphisms in temporally stable environments.

*Corresponding author. Present address: Petteri Karisto, Department of Environmental Systems Science, ETH Zürich, Universitätstrasse 2, 8092 Zürich, Switzerland; email: petteri.karisto@usys.ethz.ch.
†email: eva.kisdi@helsinki.fi

1 Introduction

For analytical tractability, many models studying the evolution of dispersal strategies assume that dispersers join a global, well mixed dispersal pool, from which they can immigrate to every patch of available habitat with equal probability (e.g. Hamilton and May 1977; Olivieri et al. 1995; Ronce et al. 1998; Gandon and Michalakis 1999; Gyllenberg and Metz 2001; Parvinen 2002; Poethke and Hovestadt 2002; Gyllenberg et al. 2011; Massol et al. 2011; etc.). In reality, however, connectivity between patches is variable, and this has an important effect on the dynamics of metapopulations (Hanski 1994; Ovaskainen and Hanski 2001). Since connectivity influences the mortality cost of dispersal, a key component of fitness of dispersal strategies, variable connectivity must have an effect also on the evolution of dispersal. Yet, apart from lattice models assuming nearest-neighbour dispersal or similar translation-invariant, symmetric rules for the connectivity between sites (e.g. Comins 1982; Harada 1999; Murrell et al. 2002; Rousset and Gandon 2002), surprisingly few models of dispersal evolution allow for variability in how well different locations are connected.

Recently, Henriques-Silva et al. (2015) conducted individual-based simulations to explore the evolution of density-dependent dispersal between populations that are the nodes of various networks. Next to a regular lattice, their networks included a random graph, an exponential network and a scale-free network, an array with increasing variability in patch connectivity, each favouring a different dispersal strategy. While this study demonstrates that variable connectivity affects dispersal evolution, it is not obvious how these networks correspond to a spatial arrangement of habitat patches, where dispersal and connectivity are subject to geometrical constraints.

Spatially realistic models, which use connectivity estimates based on the geography of real landscapes, are relevant since they incorporate natural variation in patch connectivity. The simulations of Heino and Hanski (2001) and Muneepeerakul et al. (2011) found that groups of habitat patches within the same landscape may evolve different dispersal strategies. In the butterfly metapopulation of Heino and Hanski (2001), these groups of patches are relatively isolated clusters that can maintain differences due to limited immigration. It is, however, not clear why the differences seen between the clusters evolve in the first place. Since patch areas influence local extinctions (an important driver of dispersal evolution in this model) and also scale emigration, area effects may well explain the evolution of different dispersal propensities; but differences in within-cluster connectivity may also play a role. In the river system studied by Muneepeerakul et al. (2011), the evolution of different dispersal strategies is linked to contrasting carrying capacities of the patches, with semi-isolated subnetworks playing a minor role.

North et al. (2011) used an artificial but realistic landscape to investigate the evolutionary dynamics of the width of the dispersal kernel. An evolutionarily transient (but ecologically stable) coexistence of short- and long-range dispersal strategies was possible and could be reinforced with frequent mutations, but this could be explained by patch turnover rather than connectivity (as in Olivieri et al. 1995). Bonte et al. (2010) simulated the evolution of dispersal on a lattice where suitable sites were clustered to various degrees. These simulations uncovered some local adaptation of dispersal; the width of the dispersal kernel (and therefore also the probability of leaving the site) of an individual correlated with the distribution of suitable sites in its neighbour-

hood, which indicates that sites with different connectivities favour different dispersal strategies.

Despite these hints to the effect of variable connectivity, the simulation model of Henriques-Silva et al. (2015) seems to be the only theoretical study addressing the effect of variable connectivity directly. In particular, models that incorporate some form of variable connectivity, and yet are amenable to mathematical analysis, are lacking.

Fragmented landscapes represent complex environments with habitat patches of different sizes and different connectivities at multiple spatial scales. In most models, a local population occupying a habitat patch is considered to be well mixed. In reality, however, this may not be so because competition is often localized, especially in case of plants and other sessile organisms. Moreover, a habitat patch itself is often fragmented on a smaller scale. For example, a meadow may be seen as a habitat patch for a plant, but in fact much of the meadow's area is unaccessible to the seedlings, and the offspring compete for the suitable fragments of the meadow. Since the fragments are scattered across the meadow, the seeds need to disperse within as well as between the meadows. Connectivity can thus pertain to movement on a large scale such as between separate patches, movement on a short scale such as between separate fragments within the same patch, and possibly to intermediate scales in complex landscapes.

One way to model a complex fragmented habitat is to consider it as a network of its smallest fragments, henceforth called sites. Within a site, the population is assumed to be well mixed. The sites may differ in their size, i.e., in how many individuals they contain, and how they connect to the rest of the population. Some of the sites, like the fragments of a meadow, may form a well-connected cluster, whereas others may be more isolated. We thus see the fragmented habitat as a network of sites with clusters of variable size (from a single site to many) and variable connectivity (both within and among clusters), with possibly a continuum of how strongly the clusters separate or blend in the network.

In the present paper, we simplify this complexity by assuming that the offspring compete within microsites, i.e., sites so small that each can support only one adult individual. Some microsites, such as those in the same meadow, form a large cluster, whereas other microsites are solitary with no other microsites nearby. The clustered microsites are well-connected as one can be reached from another by short-range dispersal at a relatively low cost; e.g. wind-dispersed seeds that remain close to the ground will likely remain within the meadow and will fall into a microsite with a relatively high probability. The solitary microsites are only weakly connected as they can be reached only by more costly long-range dispersal; e.g. by seeds picked up high by air currents and blown across the forest, which implies a very high probability of landing outside any microsite. This model simplifies the network of sites depicted in the previous paragraph in two different ways: first, it assumes no variation in the size of individual sites (each site supports exactly one adult), and second, it assumes only two distinct levels of connectivity (part of a large cluster vs solitary) in a spatially implicit setting.

Our model of clustered and solitary microsites is a simple and analytically tractable extension of the Hamilton–May (1977) model to variable connectivity. In the Hamilton–May model,

as in our model, the offspring compete within microsites and only one offspring survives in each site; but unlike in our model, the dispersed offspring are randomly distributed over all sites. Kin competition within the microsites selects for dispersal, whereas the mortality cost of dispersal selects against it. In the Hamilton–May model, the evolutionarily stable strategy is to disperse the fraction $d = 1/(2 - \sigma)$ of the offspring, where σ is the probability of survival during dispersal. Since in our model long-range dispersal and short-range dispersal have different mortality costs, they select for different dispersal strategies. Under contrasting selection, one may expect the evolution of a "compromise" intermediate strategy, but one may also expect that selection becomes disruptive and facilitates the evolution of dispersal polymorphisms. Using the methods of adaptive dynamics, we explore under which conditions these outcomes of dispersal evolution occur and investigate the ecological and evolutionary dynamics of dispersal polymorphisms maintained by variable connectivity.

2 The ecological model

Following the model of Hamilton and May (1977), we envisage a large population of an annual, clonal organism where each adult occupies a microsite able to support only one individual. Each adult produces B offspring and dies. The offspring disperse with probability d_k, and this probability characterizes the kth dispersal strategy ($k = 1, ..., M$). We assume large fecundity ($B \to \infty$) so that there is no demographic stochasticity during dispersal that would affect the number of non-dispersing offspring and the number of immigrants. After dispersal, the offspring compete for the site according to a fair lottery, whereby only one offspring matures and the others perish.

To include variable connectivity into a spatially implicit model, we assume that some of the microsites cluster into L large groups of well-connected sites (e.g. sites in the same meadow, which can be reached via short-range dispersal), whereas other sites are solitary (can be reached only by long-range dispersal). Of the offspring dispersed from a site of a cluster, a fraction $1 - q$ remains in a local dispersal pool, survives dispersal with probability s, and lands in a randomly chosen site within the same cluster. A fraction q of the dispersed offspring enter a global dispersal pool. The globally dispersed offspring survive dispersal with probability γs (where $0 < \gamma \leq 1$ measures the reduction in survival due to the extra hazards experienced during long-term dispersal, such as the increased risk of landing outside any site), and enter a site selected at random in the entire population. An offspring dispersed from a solitary site survives only if it enters the global dispersal pool, i.e., it survives dispersal with probability $q\gamma s$. In other words, a fraction $1 - q$ of the offspring dispersed from a solitary site perish because they engage in local dispersal only, but there are no sites they could reach with short-range dispersal; and another fraction $q(1 - \gamma s)$ engages in long-range dispersal but dies during it. Figure 1 summarizes these assumptions graphically, and Table 1 lists all variables and parameters.

Let p_1 denote the fraction of sites that are solitary and let $p_2, ..., p_{L+1}$ denote the fraction of sites that are in the L clusters ($\sum_{j=1}^{L+1} p_j = 1$). Note that we label the clusters with the indices $2, ..., L + 1$ because index 1 is reserved for the solitary sites. For the case of a single

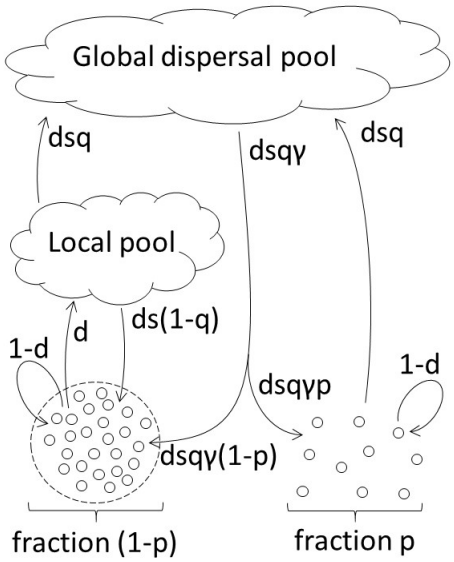

Figure 1: Variable connectivity in a spatially implicit model. Microsites (small circles) in a cluster (on the left) exchange dispersers via both a local and a global dispersal pool. Solitary sites (on the right) are accessible only via the global dispersal pool.

cluster ($L = 1$) and when the clusters can be lumped into one, we shall also write $p = p_1$ for the frequency of solitary sites and $1 - p$ for the frequency of clustered sites. In generation t, $n_{1k}(t)$ is the fraction of sites that are solitary and occupied by an adult with dispersal strategy d_k, whereas $n_{ik}(t)$ is the fraction of sites that are in cluster ($i = 2, ..., L + 1$) and occupied by strategy d_k. Note that we express population size always relative to the total number of sites (not as a fraction of solitary sites or a fraction within a cluster), such that $\sum_{k=1}^{M} n_{jk}(t) = p_j$ for $j = 1, ..., L+1$. Therefore $n_{1k}(t)/p_1$ is the fraction of solitary sites that are occupied by strategy d_k, and analogously $n_{ik}(t)/p_i$ is the frequency of strategy d_k within cluster i.

To ease the presentation of the equations governing the dynamics of this population, we first define some auxiliary variables. Let

$$I_1 = q\gamma s \sum_{j=1}^{L+1} \sum_{k=1}^{M} n_{jk} d_k \tag{1a}$$

so that $I_1 B$ is the number of immigrants per site from the global dispersal pool, and let

$$I_i = (1 - q)s \sum_{k=1}^{M} \frac{n_{ik}}{p_i} d_k \quad \text{for } i = 2, ..., L + 1 \tag{1b}$$

so that $I_i B$ is the number of immigrants to each site in cluster i from the local dispersal pool. Further, let

$$E_1 = \sum_{k=1}^{M} \frac{n_{1k}}{p_1} \cdot \frac{1}{1 - d_k + I_1} \tag{1c}$$

	Parameters
L	number of clusters
$p = p_1$	fraction of sites that are solitary
p_i	fraction of sites that are in cluster i ($i = 2, ..., L+1$)
$1-p$	fraction of sites that are in any of the clusters
s	probability of survival in the local dispersal pool (short-range dispersal)
q	probability of entering the global dispersal pool (long-range dispersal)
γ	reduction of survival in the global dispersal pool (probability of survival is γs)
B	number of offspring per adult (assumed to be large)
	Strategies
M	number of resident strategies
d_k	probability of dispersal of strategy k ($d_1 = d$ when there is only one resident)
d_{mut}	probability of dispersal of a mutant strategy
d^*	singular strategy (ESS or evolutionary branching point)
	Ecological variables
n_{1k}	fraction of sites that are solitary and occupied by strategy k
n_{ik}	fraction of sites that are in cluster i ($i = 2, ..., L+1$) and occupied by strategy k
m_1	fraction of sites that are solitary and occupied by a mutant
m_i	fraction of sites that are in cluster i ($i = 2, ..., L+1$) and occupied by a mutant
I_j, E_j	environmental feedback variables defined in equations (1)

Table 1: List of symbols

and

$$E_i = \sum_{k=1}^{M} \frac{n_{ik}}{p_i} \cdot \frac{1}{1 - d_k + I_1 + I_i} \quad \text{for } i = 2, ..., L+1 \tag{1d}$$

so that E_1/B and E_i/B are respectively the probabilities that a specific juvenile that has landed in a solitary site or in a site of cluster i wins the site during competition. Note that these auxiliary variables change in time since they depend on $n_{jk} = n_{jk}(t)$.

To calculate $n_{1k}(t+1)$, note that each solitary site occupied by an adult of strategy d_k will be occupied in the next generation by one of its own non-dispersing offspring with probability $(1-d_k)/(1-d_k+I_1)$. In addition, each of the $\sum_{j=1}^{L+1} n_{jk} B d_k$ dispersing offspring of strategy d_k enters a solitary site with probability $q\gamma s p_1$ and, upon landing, wins this site with probability E_1/B. Hence we obtain

$$n_{1k}(t+1) = \frac{1-d_k}{1-d_k+I_1} n_{1k}(t) + d_k q \gamma s p_1 E_1 \sum_{j=1}^{L+1} n_{jk}(t) \tag{2a}$$

$n_{ik}(t+1)$ for $i = 2, ..., L+1$ is calculated analogously, adding also the offspring dispersed locally

within cluster i:

$$n_{ik}(t+1) = \frac{1-d_k}{1-d_k+I_1+I_i} n_{ik}(t) + d_k s E_i \left[(1-q) n_{ik}(t) + q\gamma p_i \sum_{j=1}^{L+1} n_{jk}(t) \right] \tag{2b}$$

In appendix A we show that equations (2) have an equilibrium such that n_{ik}/p_i is the same for all $i = 2, ..., L+1$, i.e., the fraction of sites within a cluster occupied by a certain strategy k is the same in every cluster. This is because every cluster receives the same distribution of immigrants from the global dispersal pool and the same selective forces operate within every cluster. If the population settles at such a "symmetric" equilibrium, then the clusters can be pooled into a single cluster containing a fraction $1-p_1$ of all sites. Moreover, receiving the same immigrants and having the same selective forces within each cluster also imply that if there is a locally asymptotically stable equilibrium of the model with its clusters pooled into a single cluster of size $1-p_1$, then the corresponding symmetric equilibrium of the original model with L clusters is also locally asymptotically stable.

Next to its symmetric equilibrium, however, a polymorphic population may also have equilibria where n_{ik}/p_i differ among clusters ("asymmetric equilibria"). To understand this, first note that a single cluster with no immigrants from the global dispersal pool is equivalent to the Hamilton–May (1977) model. The Hamilton–May model exhibits alternative stable fixation equilibria in the following manner: there exist strategy pairs (d_1, d_2) such that a population fixed for strategy d_1 cannot be invaded by d_2 (the fixation equilibrium is transversally stable against introducing d_2 at a small initial frequency), and *vice versa*, a population fixed for d_2 cannot be invaded by d_1 (Motro 1982; Kisdi 2016). Consider now the present model with two clusters (labelled 2 and 3) and assume $p_1 = 0$, $q = 0$ so that there are no solitary sites and no globally dispersed offspring. The two clusters are then isolated, and thus one can be fixed for d_1 and the other for d_2 (in our present notation, $(n_{21}/p_2, n_{31}/p_3) = (1, 0)$). Since the fixation equilibria are asymptotically stable, there exists a stable asymmetric equilibrium $(1-\epsilon_1, \epsilon_2)$ also if the clusters are weakly coupled by global dispersal and/or receive a few immigrants from solitary sites, i.e., for sufficiently small values of q and p_1. With more than two clusters, the number of asymmetric equilibria can be high.

In this paper, we do not pursue the asymmetric equilibria further. In the next section, we investigate the adaptive dynamics of monomorphic resident populations ($M = 1$), where, irrespectively of the number of clusters L, the ecological equilibrium $n_{j1}/p_j = 1$ ($j = 1, ..., L+1$) is unique and trivial. For dimorphic resident populations in section 4, we assume that either there is only one cluster next to the solitary sites ($L = 1$) or if there are several clusters, the population is settled at the symmetric equilibrium.

3 Adaptive dynamics in monomorphic resident populations

3.1 Invasion fitness

Assume that a new mutant d_{mut} appears at a low frequency in a resident population at equilibrium. Let m_1 denote the fraction of sites that are solitary and occupied by a mutant, and let m_i $(i = 2, ..., L+1)$ be the fraction of sites that are in cluster i and are occupied by a mutant. As before, m_i/p_i is the frequency of mutants within cluster i, and $\sum_{i=1}^{L+1} m_i$ is the frequency of mutants in the population. Analogously to equations (2), the dynamics of the mutant are governed by

$$m_1(t+1) = \frac{1-d_{mut}}{1-d_{mut}+I_1} m_1(t) + d_{mut} q\gamma s p_1 E_1 \sum_{j=1}^{L+1} m_j(t) \tag{3a}$$

and, for $i = 2, ..., L+1$,

$$m_i(t+1) = \frac{1-d_{mut}}{1-d_{mut}+I_1+I_i} m_i(t) + d_{mut} s E_i \left[(1-q) m_i(t) + q\gamma p_i \sum_{j=1}^{L+1} m_j(t) \right] \tag{3b}$$

In a monomorphic resident population of strategy $d_1 = d$, the variables defined in (1) simplify to

$$\begin{aligned} I_1 &= q\gamma sd && (4a)\\ I_i &= (1-q)sd \quad \text{for } i = 2, ..., L+1 && (4b)\\ E_1 &= \frac{1}{1-d+q\gamma sd} && (4c)\\ E_i &= \frac{1}{1-d+q\gamma sd+(1-q)sd} \quad \text{for } i = 2, ..., L+1 && (4d) \end{aligned}$$

Note that in (4b) and (4d), I_i and E_i do not depend on i, i.e., all clusters provide the same environment for the mutant when the resident population is monomorphic. Mutants in the clusters can thus be pooled. Define $\tilde{m}_1 = m_1$ (fraction of sites that are solitary and occupied by a mutant individual), $\tilde{m}_2 = \sum_{i=2}^{L+1} m_i$ (fraction of sites that are in any of the clusters and occupied by a mutant), and the mutant population vector $\tilde{\mathbf{m}} = [\tilde{m}_1, \tilde{m}_2]^T$. Substituting (4) into (3) and pooling the L variables in (3b) into $\tilde{m}_2$, the linearized dynamics of the mutant (valid as long as the mutant is present only at a low frequency and can thus be neglected in (4)) can be written as $\tilde{\mathbf{m}}(t+1) = \mathbf{A}_{mut}\tilde{\mathbf{m}}(t)$ with the projection matrix

$$\begin{aligned} \mathbf{A}_{mut} &= \begin{bmatrix} a_{11} & a_{12} \\ a_{21} & a_{22} \end{bmatrix} \\ a_{11} &= \frac{1-d_{mut}}{1-d_{mut}+q\gamma sd} + \frac{d_{mut} q\gamma sp}{1-d+q\gamma sd} \\ a_{12} &= \frac{d_{mut} q\gamma sp}{1-d+q\gamma sd} \\ a_{21} &= \frac{d_{mut} q\gamma s(1-p)}{1-d+q\gamma sd+(1-q)sd} \\ a_{22} &= \frac{1-d_{mut}}{1-d_{mut}+q\gamma sd+(1-q)sd} + \frac{d_{mut} s(1-q+q\gamma(1-p))}{1-d+q\gamma sd+(1-q)sd} \end{aligned} \tag{5}$$

where $p = p_1$ is the fraction of solitary sites and $1 - p = \sum_{i=2}^{L+1} p_i$ is the fraction of sites in (any of the) clusters.

We assume $0 < p < 1$, assume that q, γ and s are strictly positive, and consider only positive, nonzero dispersal ($d_{mut} > 0$) so that the projection matrix $\mathbf{A}_{mut}$ is irreducible; note that the same assumptions also guarantee that $\mathbf{A}_{mut}$ is primitive. The invasion fitness of the mutant, λ_{mut}, is the leading eigenvalue of $\mathbf{A}_{mut}$. Because it is somewhat cumbersome to use the leading eigenvalue directly, we use instead the fitness proxy

$$F(d_{mut}, d) = \mathrm{tr}(\mathbf{A}_{mut}) - \det(\mathbf{A}_{mut}) \tag{6}$$

where tr and det denote the trace and the determinant, respectively. For 2×2 non-negative projection matrices, $F(d_{mut,}d)$ has following property:

$$\mathrm{tr}(\mathbf{A}_{mut}) \leq 2 \Rightarrow \left(F(d_{mut}, d) \gtreqless 1 \Leftrightarrow \lambda_{mut} \gtreqless 1\right)$$
$$\mathrm{tr}(\mathbf{A}_{mut}) > 2 \Rightarrow \left(\lambda_{mut} > 1, \text{ irrespectively of } F(d_{mut}, d)\right)$$

(Metz and Leimar 2011; see Kisdi 2016 for a summary). Thus the mutant can invade if $F(d_{mut}, d) > 1$ or $\mathrm{tr}(\mathbf{A}_{mut}) > 2$, and the invasion boundary $\lambda_{mut} = 1$ consists of points (d_{mut}, d) where $F(d_{mut}, d) = 1$ and $\mathrm{tr}(\mathbf{A}_{mut}) \leq 2$. Note that for d_{mut} sufficiently close to d (or, in polymorphic populations, for mutants sufficiently close to any one of the residents) the condition $\mathrm{tr}(\mathbf{A}_{mut}) \leq 2$ always holds (Metz and Leimar 2011), and therefore the fitness proxy F alone can be used to determine the evolutionary singularities and their local stability properties (see below).

Figure 2 shows a few examples of pairwise invasibility plots obtained numerically using the conditions $F(d_{mut}, d) > 1$ or $\mathrm{tr}(\mathbf{A}_{mut}) > 2$ for invasion. In each example, dispersal evolves to a unique interior evolutionarily singular strategy, which is either an ESS (as in Figure 2a,c) or an evolutionary branching point (as in Figure 2b,d; Geritz et al. 1998).

3.2 Evolutionary singularities

The evolutionary singularities are found by solving the equation

$$\left.\frac{\partial F(d_{mut}, d)}{\partial d_{mut}}\right|_{d_{mut}=d} = 0$$

for the unknown d (Geritz et al. 1998). This equation has three solutions:

$$\begin{aligned} \bar{d}_0 &= 0 \\ \bar{d}_{1,2} &= \frac{2}{3 - s(1 - q + 2q\gamma) \pm \sqrt{A/B}} \end{aligned} \tag{7}$$

where

$$\begin{aligned} A &= (1-p)(1-q)(1-(1-q)s)^2 + q\gamma\left[1 - (1-q)s(2 - 4p - (1-q)s)\right] \\ B &= (1-p)(1-q) + q\gamma \end{aligned} \tag{8}$$

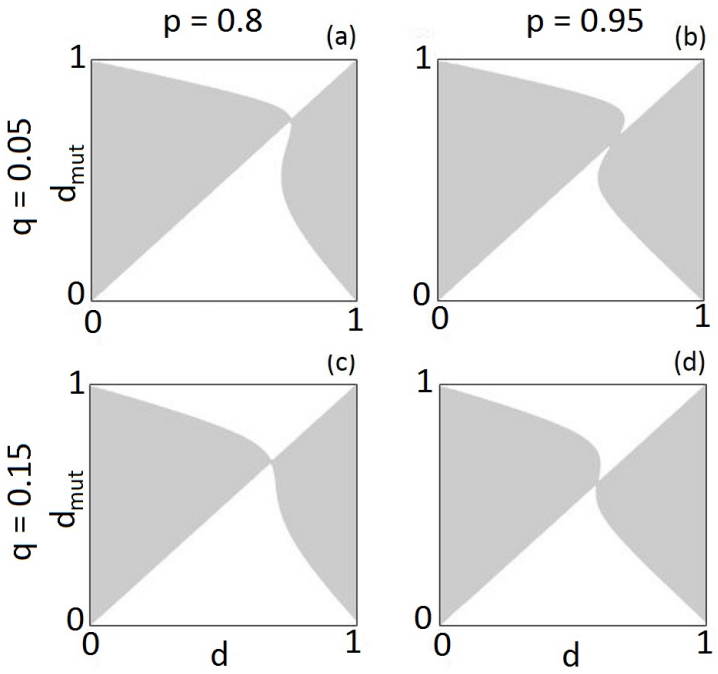

Figure 2: Pairwise invasibility plots (PIP). In the shaded areas, $\lambda_{mut} > 1$ so that the mutant can invade; in the white areas, $\lambda_{mut} < 1$ and the mutant dies out. In (a) and (c), the interior evolutionarily singular strategy is an ESS; in (b) and (d), it is an evolutionary branching point. Parameter values: $s = 0.8$, $\gamma = 0.2$, and (a) $q = 0.05, p = 0.8$; (b) $q = 0.05, p = 0.95$; (c) $q = 0.15, p = 0.8$; (d) $q = 0.15, p = 0.95$.

At the boundary solution $\bar{d}_0 = 0$, the projection matrix $\mathbf{A}_{mut}$ is reducible and hence the invasion fitness is not defined. In Appendix B, we show that when the resident dispersal strategy d is near zero, dispersal evolves towards higher values, so that $\bar{d}_0 = 0$ is always convergence unstable. In Appendix C, we prove that $\bar{d}_2$ (the root with "$-$" in front of the square root) is outside the interval $[0, 1)$, whereas $\bar{d}_1$ is a valid dispersal strategy for all possible parameter values. Since $\bar{d}_0 = 0$ is repelling, the only interior singularity, $d^* = \bar{d}_1$, is always convergence stable.

Appendix C further shows that d^* always exceeds $1/2$. This result is similar to the evolutionarily stable dispersal strategy of the Hamilton–May (1977) model, $d = 1/(2 - \sigma)$, which exceeds $1/2$ for any positive probability of survival during dispersal (σ). In our model, both limiting cases of solitary sites without clusters ($p \to 1$) and clusters without solitary sites ($p \to 0$) yield to the Hamilton–May model, albeit with different σ (when all sites are solitary, $\sigma = q\gamma s$, the probability of entering the global dispersal pool and surviving global dispersal; and when all sites are in clusters, $\sigma = q\gamma s + (1 - q)s$, the average survival of globally and locally dispersed offspring; see Appendix D). Dispersal thus evolves to exceed $1/2$ in both limiting cases, and the same remains true also when selection in solitary sites and selection in clusters are coupled.

3.3 Bifurcations of monomorphic evolutionary singularities

The unique convergence stable singularity d^* is an evolutionarily stable strategy (ESS) or an evolutionary branching point depending on whether the second partial derivative

$$\left.\frac{\partial^2 F(d_{mut}, d)}{\partial d_{mut}^2}\right|_{d_{mut}=d=d^*}$$

is negative or positive, respectively (Geritz et al. 1998). Figure 3 shows bifurcation diagrams of the monomorphic singularity indicating its evolutionary stability (shaded areas: d^* is an evolutionary branching point, white areas: d^* is evolutionarily stable).

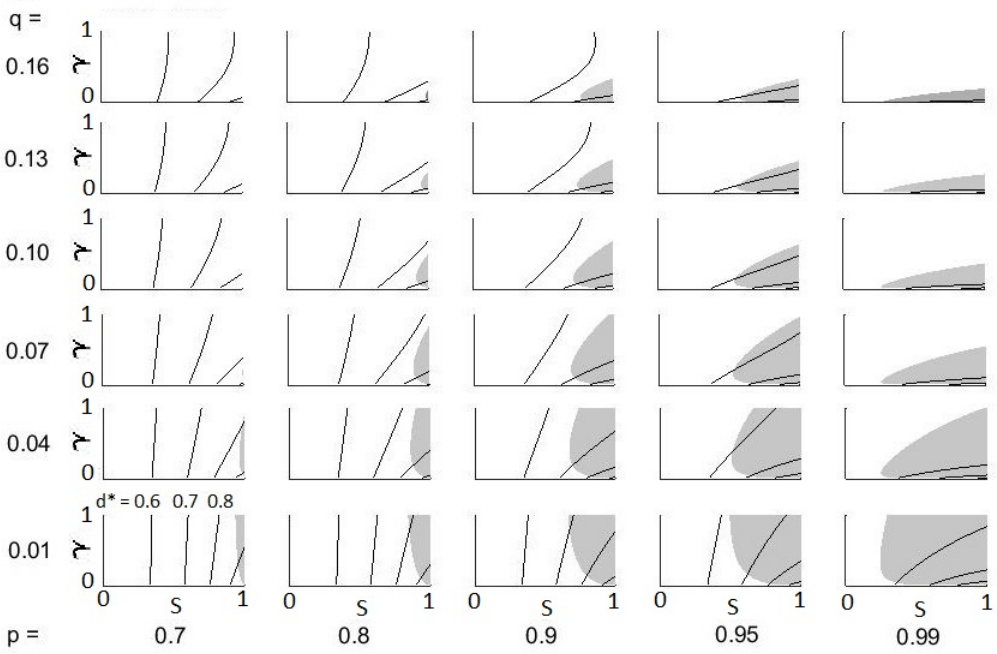

Figure 3: Bifurcations of the interior monomorphic singularity. Shaded areas: d^* is an evolutionary branching point; white areas: d^* is an ESS. The lines are contour lines of d^*; in each panel, $d^* = 0.6$ on the leftmost line (recall that $d^* > 0.5$ for all parameters) and d^* increases by 0.1 between the lines.

Evolutionary branching of dispersal is driven by contrasting selection in the well-connected sites of clusters and in the weakly connected solitary sites. As Figure 3 demonstrates, s must be sufficiently high for evolutionary branching to happen, otherwise no site (including those in the clusters) is well connected. Low values of q, the fraction of dispersers entering the global dispersal pool, and γ, the probability of surviving there relative to short-range dispersal, generally facilitate evolutionary branching because they amount to a low connectivity of solitary sites relative to the sites in the clusters. Upon closer inspection of Figure 3, increasing γ from zero to one can result in d^* bifurcating from an ESS to a branching point and then back again to an ESS, provided that q is sufficiently large. If q and γ are high, most dispersers enter the global dispersal pool and likely survive long-range dispersal, so that the solitary sites are also

well connected and the contrast with the sites in the clusters is not strong enough to obtain evolutionary branching. On the other hand, if γ is very small, then dispersers leaving solitary sites likely die (so that dispersing more offspring does not return fitness benefits) and the solitary sites hardly receive any immigrants (so that retaining more offspring in the natal site does not increase the probability that one of them wins the site, as this probability is almost 1 anyway). In this situation, selection on dispersal in the solitary sites is weak (this is analogous to the Hamilton–May (1977) model, where selection becomes vanishingly weak when the probability of surviving dispersal goes to zero), so that selection in the clusters dominates and dispersal evolves to an ESS when γ is very small.

Evolutionary branching happens only if both solitary sites and sites in the clusters are sufficiently common, otherwise a dispersal strategy favoured in the common type of sites swamps the rare sites. Therefore increasing p from zero to one can result in d^* changing from an ESS to a branching point and then back to an ESS. In Figure 3, this can be seen by comparing the panels; as p increases, a point at the same coordinates (s, γ) can be first in a white area, then in a shaded area and then in a white area again. Figure 5 in section 4 shows the effect of p and q directly and compares the region of evolutionary branching to dimorphisms. Note that a high fraction of solitary sites generally favours evolutionary branching as it prevents that the solitary sites are swamped from the clusters. Although the singularity always becomes an ESS as $p \to 1$ (see Appendix D), for low values of q and γ this happens only at p very close to 1, i.e., outside the range shown in Figure 3 and invisible in much of Figure 5. A similar bifurcation pattern from an ESS to a branching point and back to an ESS can result also when increasing q, the fraction of dispersers who enter the global pool.

4 Dimorphic populations

As explained in section 2, populations with two resident dispersal strategies, d_1 and d_2, may have many asymmetric equilibria of their population dynamics when the landscape contains several clusters. Here we initially simplify the analysis by assuming that there is ony one cluster next to the solitary sites ($L = 1$), so that the population dynamics has the four variables n_{11}, n_{12}, n_{21}, and n_{22} for the fraction of solitary and clustered sites occupied by d_1 and d_2, respectively. At the end of this section, we discuss to what extent the results generalize to several clusters.

Since the equations for the equilibrium population densities are too difficult to solve analytically, we found n_{11} and n_{21} numerically (recall that $n_{12} = p - n_{11}$ and $n_{22} = 1 - p - n_{21}$), and ascertained the asymptotic stability of this equilibrium by evaluating the Jacobian of population dynamics. We found stable coexistence equilibria both within the area of mutual invasibity (where strategies d_1 and d_2 invade each other's monomorphic population; dark shading in Figure 4) and outside of it. The latter represent unprotected dimorphisms, where a stable fixation equilibrium exists next to the locally stable coexistence equilibrium, so that a large perturbation of a dimorphic population may result in the extinction of one of the strategies (light shading in Figure 4). In the upper left corner of Figure 4, the invasion boundaries cross each other and there is a small area of mutual exclusion (both boundary equilibria of population dynamics are

stable; see inset (i)). In the neighbourhood of crossing invasion boundaries, an area of unprotected dimorphisms generically exists (Priklopil 2012).

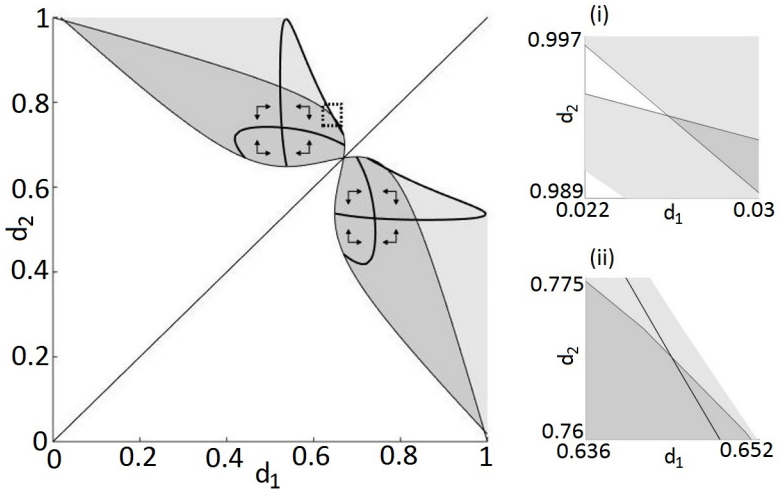

Figure 4: Adaptive dynamics in dimorphic resident populations. Dark shading: protected dimorphism (mutual invasibility), light shading: unprotected dimorphism, white: no stable coexistence. The arrows show the direction of evolution given by the selection gradients $G_1(d_1, d_2)$ (horizontal) and $G_2(d_1, d_2)$ (vertical). The thick lines are the isoclines $G_k(d_1, d_2) = 0$, and their intersection is the dimorphic singularity. The upper inset (i) shows the upper left corner of the main figure, where the invasion boundaries cross each other and there is an area of mutual exclusion (white) between the two crossing boundaries; the area of unprotected dimorphism extends also over the area of mutual exclusion. The lower inset (ii) shows the part marked with a dotted square in the main figure, where an isocline crosses the invasion boundary but remains within the area of (unprotected) coexistence. Parameter values: $s = 0.8$, $\gamma = 0.2$, $q = 0.1$, $p = 0.9$.

Once the equilibrium population densities are known, we can easily compute I_1, I_2, E_1 and E_2 defined in (1), and obtain the invasion fitness proxy of a rare mutant strategy d_{mut} as $F(d_{mut}, d_1, d_2) = \mathrm{tr}(\mathbf{A}_{mut}) - \det(\mathbf{A}_{mut})$ where, from (3) and using the notation $p_1 = p$ and $p_2 = 1 - p$, the mutant's projection matrix is

$$
\begin{aligned}
\mathbf{A}_{mut} &= \begin{bmatrix} a_{11} & a_{12} \\ a_{21} & a_{22} \end{bmatrix} \\
a_{11} &= \frac{1 - d_{mut}}{1 - d_{mut} + I_1} + d_{mut} q\gamma s p E_1 \\
a_{12} &= d_{mut} q\gamma s p E_1 \\
a_{21} &= d_{mut} q\gamma s (1-p) E_2 \\
a_{22} &= \frac{1 - d_{mut}}{1 - d_{mut} + I_1 + I_2} + d_{mut} s E_2 [1 - q + q\gamma(1-p)]
\end{aligned}
$$

By repeated invasions of mutants, the kth resident strategy ($k = 1, 2$) evolves towards higher

or lower dispersal depending on whether

$$G_k(d_1,d_2)=\left.\frac{\partial F(d_{mut},d_1,d_2)}{\partial d_{mut}}\right|_{d_{mut}=d_k}$$

is positive or negative (Geritz et al. 1998; the arrows in Figure 4 show the direction of evolution). The interior evolutionary singularity of a dimorphic population, (d_1^*,d_2^*), is determined by the equations $G_k(d_1^*,d_2^*)=0$ for $k=1,2$. In Figure 4, the dimorphic singularity is shown by the intersection of the isoclines of $G_k(d_1^*,d_2^*)=0$, across which the direction of evolution changes. The dimorphic singularity is evolutionarily stable if

$$\frac{\partial^2 F(d_{mut},d_1^*,d_2^*)}{\partial d_{mut}^2}<0 \tag{9}$$

holds for both $d_{mut}=d_1^*$ and $d_{mut}=d_2^*$.

To establish the convergence stability of a dimorphic singularity, we use the concept of strong convergence stability (Leimar 2009) applied to polymorphic populations with scalar traits as follows (see also Kisdi and Geritz 2016). We approximate the joint adaptive dynamics of the two residents with the canonical equation

$$\begin{aligned}\dot{d}_1 &= \kappa_1(d_1,d_2)G_1(d_1,d_2)\\ \dot{d}_2 &= \kappa_2(d_1,d_2)G_2(d_1,d_2)\end{aligned}$$

where the dot denotes the time derivative on the evolutionary time scale (Dieckmann and Law 1996; Durinx et al. 2008). $\kappa_1,\kappa_2>0$ are (unknown) speed factors that combine two different effects: (i) the frequency and phenotypic size of mutations, as derived by Dieckmann and Law (1996) and Durinx et al. (2008); and (ii) a positive conversion factor that arises because $G_k(d_1,d_2)$ is based on the fitness proxy F rather than on the invasion fitness itself, and therefore $G_k(d_1,d_2)$ is sign-equivalent to the selection gradient of the kth strategy (which should appear on the right hand side of the canonical equation) but numerically not equal to it. Note that the speed factors depend on the resident strategies because the frequency of mutations the kth resident receives depends on its population size, which in turn depends on d_1 and d_2; and because the conversion from the fitness proxy to the selection gradient varies with the entries of the mutant projection matrix, which again depend on d_1 and d_2.

The dimorphic singularity is strongly convergence stable if it is an asymptotically stable fixed point of the canonical equation for every choice of positive speed factors. This is the case if the 2×2 Jacobian of the canonical equation

$$\left[\begin{array}{cc}\kappa_1\frac{\partial G_1}{\partial d_1} & \kappa_1\frac{\partial G_1}{\partial d_2}\\ \kappa_2\frac{\partial G_2}{\partial d_1} & \kappa_2\frac{\partial G_2}{\partial d_2}\end{array}\right]_{d_1=d_1^*,d_2=d_2^*}$$

has a negative trace and a positive determinant for any $\kappa_1(d_1^*,d_2^*),\kappa_2(d_1^*,d_2^*)>0$, i.e., the dimorphic singularity (d_1^*,d_2^*) is strongly convergence stable if the conditions

$$\frac{\partial G_1}{\partial d_1}<0,\ \frac{\partial G_2}{\partial d_2}<0 \quad\text{and}\quad \frac{\partial G_1}{\partial d_1}\frac{\partial G_2}{\partial d_2}>\frac{\partial G_1}{\partial d_2}\frac{\partial G_2}{\partial d_1} \tag{10}$$

hold at (d_1^*, d_2^*).

We explored the dimorphic singularities using a numerical continuation procedure. Starting with the parameters $\gamma = 0.01$, $q = 0.01$, $p = 0.99$ and $s = 0.99$ (a parameter set conducive to dimorphisms), we gradually changed the value of γ and tracked the dimorphic singularity as long as it existed; then for each such value of γ, we varied q; then for each pair of γ and q, we varied p; and finally s, with stepsize 0.03 in every direction. (Note that this procedure may miss some dimorphic singularities.)

All dimorphic singularities we found in our numerical analysis were both evolutionarily stable and strongly convergence stable. The dimorphic singularity therefore does not undergo any bifurcation of the evolutionary dynamics. The dimorphic singularity was also always in the area of protected dimorphism. With changing parameters, the dimorphic singularity can cross the lower boundary of the coexistence area (the boundary between dark shading and white in Figure 4) and therefore be lost as a biologically feasible dimorphism. This happens through a transcritical bifurcation of the population dynamic equilibrium of the singular dimorphism, whereby the lower dispersal strategy goes extinct.

Figure 5 shows in which part of the parameter space we found an evolutionarily stable dimorphism (marked with dots). Generally, parameter values that imply a large contrast between the connectivity of solitary sites and that of the sites in the cluster are conducive to the existence of a dimorphic singularity. This is the case for low values of q and γ, i.e., when the connectivity of solitary sites is weak because only few of the dispersers enter the global dispersal pool and even fewer survive there. High values of s are necessary because otherwise all dispersers have only a small probability of survival so that all sites are only weakly connected. Finally, a sufficiently large fraction of the sites should be solitary (high p) for a dimorphic singularity to exist so that the solitary sites are not swamped by dispersers from the cluster.

These conditions are qualitatively similar to those promoting evolutionary branching (see section 3.3), but the parameter combinations where evolutionary branching occurs and where a dimorphic singularity exists do not coincide. A dimorphic singularity always exists when the monomorphic population has an evolutionary branching point, but there is also a large part of parameter space where an evolutionarily stable dimorphism exists but a monomorphic population evolves to an ESS (Figure 5; Geritz et al. 1999).

In Figure 6, we vary one parameter at a time and show the effect on the dispersal strategies of the evolutionarily stable dimorphism (panel (a)) and on the population dynamic equilibrium of the singular dimorphism (panel (b)). As expected, the greater the contrast between the connectivity of sites (lower values of q and γ, higher values of s), the greater is the difference between the two dispersal strategies of the evolutionarily stable dimorphism (Figure 6a). In Figure 6b, all points are below the identity line ($n_{11}/p > n_{21}/(1-p)$), which means that the low-dispersal strategy d_1^* is more frequent among individuals occupying the solitary sites than among those who live in the cluster. This is in accordance with the Hamilton–May (1977) model; since dispersal from the solitary sites is more dangerous, lower dispersal is favoured in the solitary sites

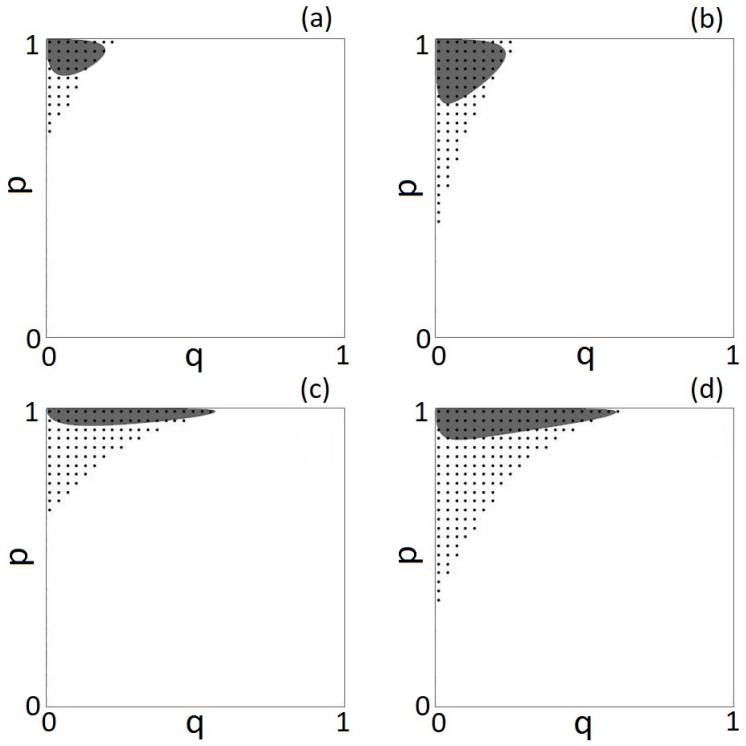

Figure 5: Evolutionarily stable dimorphisms vs evolutionary branching. The dots mark parameter combinations where an evolutionarily stable dimorphism exists. The grey background shading shows where the monomorphic evolutionary singularity is a branching point (similarly to Figure 3). Notice that the parameter region with evolutionarily stable dimorphism covers the region of evolutionary branching but also extends well beyond it. (a) $s = 0.75$, $\gamma = 0.16$; (b) $s = 0.9$, $\gamma = 0.16$; (c) $s = 0.75$, $\gamma = 0.01$; (d) $s = 0.9$, $\gamma = 0.01$.

(but see the Discussion on contrasting forces of selection).

As the contrast between the connectivity of sites decreases (higher q and γ, lower s), the low-dispersal strategy becomes less frequent in the solitary sites (n_{11}/p decreases) and initially more frequent in the cluster ($n_{21}/(1-p)$ increases; see the right half of Figure 6b), i.e. the difference between the solitary sites and the cluster diminishes. This happens because there is more dispersal between the solitary sites and the cluster, but also because the dispersal probability of the low-dispersal strategy increases (Figure 6a) and therefore it is less strongly selected against in the cluster. Yet its presence in the cluster depends on the immigrants from the solitary sites, where the low-dispersal strategy is favoured. As the contrast between the connectivities further decreases and the low-dispersal strategy is no longer common in the solitary sites, immigration can no longer support its population in the cluster. The frequency of the low-dispersal strategy therefore declines also in the cluster (left half Figure 6b), and eventually the dimorphism is lost when the low-dispersal strategy goes extinct and the hump-shaped curves in Figure 6b arrive at the origin.

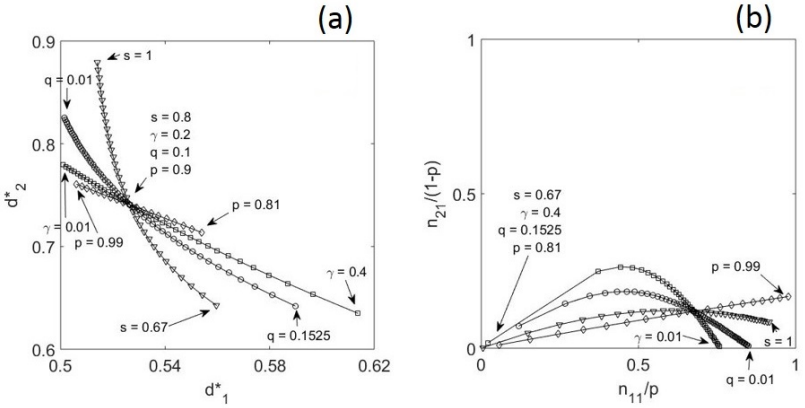

Figure 6: Changes in the dispersal strategies of the evolutionarily stable dimorphism (a) and in the population dynamic equilibrium (b) when varying the four model parameters p, s, q, γ. We label the strategy with lower dispersal as strategy 1 and the one with higher dispersal as strategy 2. Each curve varies one parameter with steps of size 0.01, except q for which the stepsize is 0.0025, omitting the points $p = 1$, $q = 0$ and $\gamma = 0$ because these have been excluded by assumption (see section 3). The parameter values written at the endpoints of the curves indicate the range of each parameter for which a dimorphic singularity exists, cf. Figure 5 (in panel (b), values belonging to the endpoints near the origin had to be lumped for readability). Non-varied parameters take the values used in Figure 4, $s = 0.8$, $\gamma = 0.2$, $q = 0.1$, $p = 0.9$ (at these values all curves intersect). Notice the different scales of the axes in (a). For (b), recall that $n_{12}/p = 1 - n_{11}/p$ and $n_{22}/(1-p) = 1 - n_{21}/(1-p)$.

Consider now a landscape with an arbitrary number of clusters next to the solitary sites. If the population is at its symmetric equilibrium (see section 2), then the clusters can be lumped into one, similarly to the monomorphic case (section 3.1). The so-called Tube Theorem of Geritz et al. (2002) ensures that the population remains at the symmetric equilibrium and therefore one can continue lumping the clusters as the resident strategies evolve by small mutational steps, provided that the symmetric equilibrium remains stable. In section 2 we argued that the latter condition is satisfied whenever the lumped model with only one cluster has a stable equilibrium. Hence we can apply the results of this section directly to a model with L clusters: if the initial population is at the symmetric equilibrium, then the selection gradients, the dimorphic evolutionary singularity and its stability properties are the same as in case of a single cluster equivalent in size to the L clusters together. Moreover, since the pairwise invasibility plot is the same for L clusters as in the lumped model with one cluster (section 3.1), the set of protected dimorphisms (dark shaded area in Figure 4) is also the same. The unprotected dimorphisms may, however, be different.

5 Discussion

Variable connectivity must be the norm at all spatial scales in populations occupying fragmented habitats. In this paper, we have found that variable connectivity between microsites can facil-

itate the diversification of dispersal strategies and can maintain evolutionarily stable dispersal polymorphisms. We used a simple, mathematically tractable model with two contrasting levels of connectivities (solitary sites and sites in large clusters; Figure 1). Evolutionary branching and evolutionarily stable dimorphisms are favoured generally by the same conditions, i.e., high contrast between connectivities and many solitary sites. While the existence of the clusters is essential, dispersers from the cluster easily swamp the solitary sites, so that diversity occurs most easily when most sites are solitary (cf. Figures 3 and 5).

Concerning the evolution of monomorphic populations, the analysis of our model is complete. We have shown that there exists a unique interior singularity which is always convergence stable, we have obtained the location of this singularity explicitly, and determined analytically whether it is an ESS or an evolutionary branching point (Figure 3).

The analysis of dimorphic adaptive dynamics is complicated by the "asymmetric" equilibria of the resident population (see Section 2). Assuming either that all well-connected sites form a single cluster (in which case there are no asymmeric equilibria) or the population is at its symmetric equilibrium, we found that all singular dimorphisms are protected, convergence stable, and also evolutionarily stable, i.e., no further branching occurs into trimorphisms. This however does not exclude the existence of trimorphisms, and a trimorphism might even be evolutionarily stable (analogously to the simultaneous existence of a monomorphic ESS and an evolutionarily stable dimorphism, see Figure 5 and Geritz et al. 1999). The number of potentially coexisting strategies is bounded by the number of environmental feedback variables, i.e., the number of quantities through which the resident population affects the invasion dynamics of a mutant (Levin 1970; Metz et al. 1992; Geritz et al. 1997; Meszéna et al. 2006). In the present model with one cluster ($L = 1$), there are four environmental feedback variables, I_1, I_2, E_1, and E_2, which appear in the mutant dynamics in equations (3). Hence this upper bound would allow also for three or four coexisting dispersal strategies, a possibility we did not explore.

5.1 Selective forces under variable connectivity vs variable patch size

The present model is simplified from a model depicting a fragmented landscape as a network of sites with variable size and connectivity (see Introduction). Recall that by definition, we call a fragment of the habitat a "site" if it is internally well mixed. In models with variable patch size (such as Massol et al. 2011; Kisdi 2016), a patch corresponds to a well-mixed site. In these models, the sites differ in the number of individuals they support but not in their connectivity. In contrast, the present model assumes that every site supports exactly one individual but the sites have different connectivity (similar to the model of Henriques-Silva et al. (2015), who set the same finite carrying capacity for every site and varied their connectivity according to different rules of network generation). The clusters of our model are different from the patches of previous models because the clusters are internally structured into microsites, and competition happens separately within each microsite. As we argued in the Introduction, what physically appears as a habitat patch (e.g. a meadow) is often not well-mixed and is better described as a cluster of microsites connected by short-range dispersal.

Models with variable patch size predict evolutionary branching of dispersal (Massol et al. 2011; Kisdi 2016) and predict that in polymorphic populations, low-dispersal strategies are common in large patches and high-dispersal strategies are favoured in small patches (Kisdi 2016; Fig. 3 of Laroche et al. 2016). This is easy to understand in terms of the underlying selective forces; costly dispersal is favoured where kin competition is strong, i.e., in small patches where many of the competitors are siblings, but it is disfavoured in large patches where it has no benefit. In the model of Massol et al. (2011) and Laroche et al. (2016), high-dispersal strategies are further disfavoured in large patches by the large patches being sources and the small patches being sinks; this source–sink structure is not present in the model of Kisdi 2016 and in the present model. In contrast to models with variable patch size, the present model of variable connectivity predicts that the high-dispersal strategy is common in the large clusters and the low-dispersal strategy is common among the solitary sites (Figure 6b shows that the frequency of the low-dispersal strategy among the solitary sites, on the horizontal axis, always exceeds its frequency in the clusters, on the vertical axis).

This equilibrium represents a balance between three selective forces (cf. Gandon and Michalakis 1999). First, by staying in its natal microsite, an offspring increases the probability that this site will be occupied by one of the siblings born in that site rather than by an unrelated immigrant. The importance of this, however, depends on the number of immigrants. If no immigrant arrived at the site, then the best strategy would be to disperse all but one offspring, because all but one non-dispersed offspring would succumb to kin competition. Similarly, if few immigrants arrive at the site, then the probability of retaining the site for the family quickly saturates with the number of non-dispersed offspring and thus many of the offspring should be dispersed. If, however, many immigrants arrive at the site and dilute competition among kin, then the probability of retaining the site for the family saturates only slowly with the number of non-dispersed siblings, and therefore low dispersal is favoured. Solitary sites receive fewer immigrants both because only part of the dispersers travel long-range and because many of those who do, die en route. Therefore, this first factor selects for higher dispersal in solitary sites relative to the well-connected sites of the clusters, the opposite of the pattern we found.

By dispersing, an offspring has a chance to win a microsite elsewhere. This chance depends on the probability of surviving dispersal and on the number of competitors encountered in the site where the offspring arrives. An offspring leaving a solitary site has a high probability of dying during dispersal (either could not engage in long-range dispersal or died during it), thus this second factor selects for lower dispersal in solitary sites relative to the clusters. Offspring dispersing from well-connected sites have a higher probability to land in another well-connected site, where they encounter more competitors than in a solitary site; this third factor implies a lower benefit from dispersal and therefore selects for lower dispersal in well-connected sites relative to solitary sites.

Taken together, the first and third factors of selection favour higher dispersal in solitary sites, but are, in our model, overpowered by the second factor. The spatial distribution of high- and low-dispersal strategies is thus predominantly determined by the costs of dispersal, and since offspring dispersing from well-connected sites pay a lower cost, high dispersal is favoured in the well-connected sites of the clusters. This pattern is different from the prediction of models

assuming variable patch size, because the clusters of our model are internally structured into microsites, and dispersal within a cluster is necessary to avoid kin competition by moving between the clustered microsites.

5.2 Limiting cases

In the Hamilton–May (1977) model, dispersal evolves to a unique evolutionarily and convergence stable strategy. We recover this result in four different limiting cases of our model: (i) $q = 1$, every dispersed offspring enters the global dispersal pool and hence every site is equally connected to every other site; (ii) $p \to 0$ or (iii) $p \to 1$ so that all sites are of the same type; and (iv) $q\gamma \to 0$, the solitary sites are unreachable. In Appendix D, we analyze these four limiting cases in detail. In cases (i) and (ii), we show that the invasion fitness of our model converges to that of the Hamilton–May (1977) model, and therefore the pairwise invasibility plot as well as the evolutionary singularity and its stability properties are the same as in the Hamilton–May model. In cases (iii) and (iv), however, the convergence of models is only local; the evolutionary singularity of our model and its stability properties converge to those of the Hamilton–May model, but the pairwise invasibility plot remains different (see Figure 7 in Appendix D). In particular, coexistence remains possible also in the limit, even though the Hamilton–May model admits no coexistence (see Motro 1982). For (iii) $p \to 1$, the reason for this is that even if almost every site is solitary, there are still infinitely many sites in the clusters, and these can support a locally adapted dispersal strategy. In case (iv) $q\gamma \to 0$, the almost perfect isolation of solitary sites and clusters makes coexistence possible. A similar situation of local, but not global, convergence of the pairwise invasibility plots was found also in the model of Kisdi (2016). The biological significance of this limiting behaviour is that the presence of a cluster can maintain dispersal polymorphism (but not evolutionary branching) even if an arbitrarily high fraction of microsites is solitary; but the presence of solitary sites cannot do the same if the majority of sites are clustered.

Even though the singularity becomes an ESS in the limit $p \to 1$, a high fraction of solitary sites favours evolutionary branching and the bifurcation point between an ESS and evolutionary branching can exceed $p = 0.99$ (Figures 3 and 5). Since evolutionary branching is driven by the contrast between solitary and well-connected sites, both must be sufficiently common for evolutionary branching to happen; this parallels the finding that in models with variable patch size, evolutionary branching happens when both small and large patches contain a sufficiently high fraction of the population (Massol et al. 2011; Kisdi 2016). Yet in our model, a small fraction of well-connected sites is often sufficient for evolutionary branching. This is different from the case of variable patch size, where the small and large patches have to be more balanced (see Fig. 2 of Kisdi 2016).

5.3 Model assumptions revisited

For the sake of analytical tractability, we assumed a very simple spatial structure with well connected vs solitary microsites each supporting only one adult. These assumptions could be relaxed in many interesting directions. First, allowing for variation not only in connectivity but

also patch size would yield a more realistic model of fragmented landscapes.

Further, if different clusters had different internal connectivity, then in isolation they would select for different dispersal strategies as each would correspond to the Hamilton–May (1977) model but with different survival probability. A network with such clusters weakly connected by long-range dispersal would be akin to models of local adaptation to contrasting environments with weak coupling between the different habitats, a situation conducive to evolutionary branching.

If clusters were small (i.e., contained only finitely many microsites), then siblings dispersed within the cluster would have a chance to end up in the same microsite after dispersal, so that there would be kin competition also among the dispersed offspring. Dispersed offspring would also have a positive probability of returning to their site of origin (both possibilities are excluded in our model in Eqs. (2)). As long as these effects are present, selection within the cluster depends on the size of the cluster, and therefore with sufficiently weak coupling via global dispersal, clusters of different size could maintain different, locally adapted dispersal strategies. As the number of microsites in the clusters goes to infinity, these effects vanish and selection within the clusters becomes asymptotically independent of the relative size of the clusters. This fact underpins pooling the clusters at the symmetric equilibrium (see section 2), and it is analogous to the fact that the ESS of the Hamilton–May (1977) model is independent of the number of sites.

As in the Hamilton–May (1977) model, we assumed that every microsite is occupied at reproduction, i.e., there is no mortality after competition but before reproduction. In reality, however, there would be sites where the occupant dies before it would produce offspring. The presence of sites without non-dispersed offspring selects for higher dispersal (because of low post-dispersal competition in these sites; Comins et al. 1980) and facilitates the coexistence of dispersal strategies (Weigang and Kisdi 2015), but in itself, it does not lead to evolutionary branching (Appendix A of Weigang and Kisdi 2015).

In our model, the propensity to disperse (d) evolves, but the probability of long- vs short-range dispersal (q) is considered to be constant. However, the traits of an offspring that influence the probability of dispersal (e.g. the presence and morphology of seed wings or pappi) may well influence also whether the offspring remains in the local dispersal pool or travels afar. The following argument shows that evolving q instead of d would likely also result in evolutionary branching. If we take $s = 1$ and $d = 1$ (fixed) in the present model, evolve q, and, contrary to section 2, assume that dispersers leaving a solitary site but failing to enter the global dispersal pool return safely to their site of origin, then we recover the variable patch-size model of Kisdi (2016), with our present q being the probability of dispersal and γ being the probability of survival during dispersal in Kisdi (2016). With $s = 1$ and $d = 1$, the cluster of our model becomes the well-mixed patch of Kisdi (2016) because all offspring leave the microsites and those who remain within the cluster are well-mixed at no cost. Since dispersal undergoes evolutionary branching in Kisdi's model, q must undergo evolutionary branching in our model if s and d are sufficiently close to 1 and we change the assumption that short-range dispersers from solitary sites perish. If γ is small, then this change probably does not make a large difference, because

leaving a solitary site is very risky whether or not failing to enter the global dispersal pool is fatal. Hence we expect that q could undergo evolutionary branching also in our original model, yielding two strategies specialized for short-range and long-range dispersal. Note that a similar comparison of our model with the variable patch-size model of Massol et al. (2011) is not possible because their model has a source-sink structure among patches of different sizes which is not present here.

6 Conclusion

A number of previous models have predicted diversity in dispersal strategies, but most of these assume that non-equilibrium population dynamics, driven either internally or by environmental stochasticity, maintain dispersal (e.g. Doebeli and Ruxton, 1997; Mathias et al., 2001; Parvinen, 2002). Our work adds to a growing list of models demonstrating that in stable environments, kin competition can maintain not only dispersal (as shown by Hamilton and May, 1977) but also dispersal polymorphisms. Weigang and Kisdi (2015) introduced post-competitive mortality and a non-linear trade-off into the HamiltonMay (1977) model, and showed that the former facilitates coexistence and the latter can then lead to disruptive selection on coexisting dispersal strategies, i.e., to evolutionary branching. Environmental heterogeneity is a straightforward mechanism facilitating diversification. When kin competition maintains dispersal, two important factors are the size of well-mixed habitat patches (and therefore the strength of kin competition) and the connectivity between these sites (and therefore dispersal mortality). The simple HamiltonMay (1977) model assumes both to be homogeneous. Massol et al. (2011) and Kisdi (2016) have shown that heterogeneity in patch size can lead to evolutionary branching of dispersal, whereas the present model shows that heterogeneity in connectivity can do the same.

Acknowledgements

We thank three anonymous reviewers for their helpful comments. This research was financially supported by the Academy of Finland through the Centre of Excellence in Analysis and Dynamics.

References

Bonte D., T. Hovestadt & H.-J. Poethke. 2010. Evolution of dispersal polymorphism and local adaptation of dispersal distance in spatially structured landscapes. Oikos 119: 560-566.

Comins H. N. 1982. Evolutionarily stable strategies for localized dispersal in two dimensions. J. Theor. Biol. 94: 579-606.

Comins H. N., W. D. Hamilton & R. M. May. 1980. Evolutionarily stable dispersal strategies. J. Theor. Biol. 32:205-230.

Dieckmann U. & R. Law. 1996. The dynamical theory of coevolution: A derivation from stochastic ecological processes. J. Math. Biol. 34:579-612.

Doebeli M. & G. D. Ruxton. 1997. Evolution of dispersal rates in metapopulation models: Branching and cyclic dynamics in phenotype space. Evolution 51: 1730-1741.

Durinx M., J. A. J. Metz & G. Meszéna. 2008. Adaptive dynamics for physiologically structured population models. J. Math. Biol. 56: 673-742.

Gandon S. & Y. Michalakis. 1999. Evolutionarily stable dispersal rate in a metapopulation with extinctions and kin competition. J. Theor. Biol. 199: 275-290.

Geritz S. A. H., M. Gyllenberg, F. J. A. Jacobs & K. Parvinen. 2002. Invasion dynamics and attractor inheritance. J. Math. Biol. 44:548-560.

Geritz, S. A. H., É. Kisdi, G. Meszéna & J. A. J. Metz. 1998. Evolutionarily singular strategies and the adaptive growth and branching of the evolutionary tree. Evol. Ecol. 12: 35-57.

Geritz S. A. H., J. A. J. Metz, E. Kisdi & G. Meszéna. 1997. Dynamics of adaptation and evolutionary branching. Phys. Rev. Lett. 78: 2024-2027.

Geritz, S. A. H., E. van der Meijden & J. A. J. Metz. 1999. Evolutionary dynamics of seed size and seedling competitive ability. Theor. Pop. Biol. 55: 324-343.

Gyllenberg M., E. Kisdi & M. Utz. 2011. Body condition dependent dispersal in a heterogeneous environment. Theor. Pop. Biol. 79: 139-154.

Gyllenberg M. & J. A. J. Metz. 2001. On fitness in structured metapopulations. J. Math. Biol. 43: 545-560.

Hamilton W. D. & R. M. May. 1977. Dispersal in stable habitats. Nature 269: 578-581.

Hanski I.1994. A practical model of metapopulation dynamics. J. Anim. Ecol. 63:151-162.

Harada Y. 1999. Short- vs. long-range disperser: The evolutionarily stable allocation in a lattice-structured habitat. J. Theor. Biol. 201:171-187.

Heino M. & I. Hanski. 2001. Evolution of migration rate in a spatially realistic metapopulation model. Am. Nat. 157: 495-512.

Henriques-Silva R., F. Boivin, V. Calgano, M. C. Urban & P. R. Peres-Neto. 2015. On the evolution of dispersal via heterogeneity in spatial connectivity. Proc. R. Soc. B 282: 20142879.

Kisdi É. 2016. Dispersal polymorphism in stable habitats. J. Theor. Biol. 392: 69-82.

Kisdi É. & S. A. H. Geritz. 2016. Adaptive dynamics of saturated polymorphisms. J. Math. Biol. 72: 1039-1079.

Laroche F., P. Jarne, T. Perrot & F. Massol. 2016. The evolution of the competition-dispersal trade-off affects α- and β-diversity in a heterogeneous metacommunity. Proc. R. Soc. B 283: 20160548.

Leimar O. 2009. Multidimensional convergence stability. Evol. Ecol. Res. 11: 191-208.

Levin S. A. 1970. Community equilibria and stability, and an extension of the competitive exclusion principle. Am. Nat. 104: 413-423.

Massol F., A. Duputié, P. David & P. Jarne. 2011. Asymmetric patch size distribution leads to disruptive selection on dispersal. Evolution 65: 490-500.

Mathias A., E. Kisdi & I. Olivieri. 2001. Divergent evolution of dispersal in a heterogeneous and variable landscape. Evolution 55: 246-259.

Meszéna G., M. Gyllenberg, L. Pásztor & J. A. J. Metz. 2006. Competitive exclusion and limiting similarity: A unified theory. Theor. Pop. Biol. 69: 68-87.

Metz J. A. J. & O. Leimar. 2011. A simple fitness proxy for structured populations with continuous traits, with case studies on the evolution of haplo-diploids and genetic dimorphisms. J. Biol. Dyn. 5: 163-190.

Metz J. A. J., R. M. Nisbet & S. A. H. Geritz, 1992. How should we define 'fitness' for general

ecological scenarios? Trends Ecol. Evol. 7:198-202.

Motro U. 1982. Optimal rates of dispersal. I. Haploid populations. Theor. Pop. Biol. 21: 394-411.

Muneepeerakul R., S. Azaele, S. A. Levin, A. Rinaldo & I. Rodriguez-Iturbe. 2011. Evolution of dispersal in explicitly spatial metacommunities. J. Theor. Biol. 269: 256-265.

Murrell D. J., Travis J. M. J. & C. Dytham. 2002. The evolution of dispersal distance in spatially-structured populations. Oikos 97: 229-236.

North A., S. Cornell & O. Ovaskainen. 2011. Evolutionary responses of dispersal distance to landscape structure and habitat loss. Evolution 65: 1739-1751.

Olivieri I., Y. Michalakis & P.-H. Gouyon. 1995. Metapopulation genetics and the evolution of dispersal. Am. Nat. 146: 202-228.

Ovaskainen O. & I. Hanski. 2001. Spatially structured metapopulation models: Global and local assessment of metapopulation capacity. Theor. Pop. Biol. 60: 281-302.

Parvinen K. 2002. Evolutionary branching of dispersal strategies in structured metapopulations. J. Math. Biol. 45: 106-124.

Priklopil T. 2012. On invasion boundaries and the unprotected coexistence of two strategies. J. Math. Biol. 64: 1137-1156.

Poethke H. J. & T. Hovestadt. 2002. Evolution of density- and patch-size-dependent dispersal rates. Proc. R. Soc. Lond. B 269: 637-645.

Ronce O., J. Clobert & M. Massot. 1998. Natal dispersal and senescence. Proc. Natl. Acad. Sci. U.S.A. 95: 600-605.

Rousset F. & S. Gandon. 2002. Evolution of the distribution of dispersal distance under distance-dependent cost of dispersal. J. Evol. Biol. 15: 515-523.

Weigang H. C. & E. Kisdi. 2015. Evolution of dispersal under a fecundity-dispersal trade-off. J. Theor. Biol. 371: 145-153.

Appendix A

In this Appendix, we prove the existence of a symmetric equilibrium of the population dynamics in equations (2), i.e., an equilibrium where $n_{2k}/p_2 = n_{3k}/p_3 = ... = n_{L+1,k}/p_{L+1}$ for $k = 1, ..., M$. Let $f_{ik} = n_{ik}/p_i$ denote the frequency of strategy d_k within cluster i for $i = 2, ..., L+1$ or among the solitary sites for $i = 1$. Further, let $x_k = \sum_{i=1}^{L+1} n_{ik} = \sum_{i=1}^{L+1} p_i f_{ik}$ be the frequency of strategy k in the entire population. By dividing equation (2a) with p_1 and (2b) with p_i, and taking $n_{ik}(t+1) = n_{ik}(t) = n_{ik}$ for equilibrium, we obtain

$$f_{1k} = \frac{1-d_k}{1-d_k+I_1} f_{1k} + d_k q\gamma s E_1 x_k$$

and

$$f_{ik} = \frac{1-d_k}{1-d_k+I_1+I_i} f_{ik} + d_k s E_i \left[(1-q) f_{ik} + q\gamma x_k\right]$$

Substituting

$$I_i = (1-q)s \sum_{j=1}^{M} f_{ij} d_j$$

$$E_1 = \sum_{l=1}^{M} \frac{f_{1l}}{1-d_l+I_1}$$

$$E_i = \sum_{l=1}^{M} \frac{f_{il}}{1-d_l+I_1+I_i}$$

from (1b), (1c) and (1d), we arrive at

$$f_{1k} = \frac{1-d_k}{1-d_k+I_1} f_{1k} + d_k q\gamma s \sum_{l=1}^{M} \frac{f_{1l}}{1-d_l+I_1} x_k \tag{A.1a}$$

and

$$\begin{aligned} f_{ik} = \quad & \frac{(1-d_k) f_{ik}}{1-d_k+I_1+(1-q)s\sum_{j=1}^{M} f_{ij} d_j} + \\ & + d_k s \left[\sum_{l=1}^{M} \frac{f_{il}}{1-d_l+I_1+(1-q)s\sum_{j=1}^{M} f_{ij} d_j}\right] \left[(1-q) f_{ik} + q\gamma x_k\right] \end{aligned} \tag{A.1b}$$

for $i = 2, ..., L+1$, where, from (1a), $I_1 = q\gamma s \sum_{j=1}^{M} x_j d_j$.

The following proof rests on the fact that the right hand side of (A.1b) does not depend on i in any other way than through the f_{ij}'s, i.e., the equilibrium condition is the same for each cluster. However, the right hand side of (A.1b) also depends on $x_k = \sum_{i=1}^{L+1} p_i f_{ik}$, which, though does not create a difference between the clusters, couples the equations across all clusters and the solitary sites.

We therefore proceed in two steps. First, suppose that the x_k's, collected in the M-vector $\mathbf{x} = [x_1, ..., x_M]$, are fixed; this also fixes the value of I_1. Let $\boldsymbol{\phi} \in S_M$ be an M-vector of frequencies i.e., a vector in the M dimensional simplex $S_M = \{[z_1, ..., z_M] : z_i \geq 0 \text{ for all } i \text{ and } \sum_{i=1}^M z_i = 1\}$ and let

$$\begin{aligned}\Phi_k(\boldsymbol{\phi}) = \quad & \frac{(1-d_k)\phi_k}{1-d_k+I_1+(1-q)s\sum_{j=1}^M \phi_j d_j} + \\ & + d_k s \left[\sum_{l=1}^M \frac{\phi_l}{1-d_l+I_1+(1-q)s\sum_{j=1}^M \phi_j d_j}\right] [(1-q)\phi_k + q\gamma x_k]\end{aligned}$$

where the right hand side is exactly like in (A.1b), except that ϕ_j replaces f_{ij} for all j. It is easily verified that $\sum_{k=1}^M \Phi_k(\boldsymbol{\phi}) = \sum_{l=1}^M \phi_l = 1$, i.e., the (continuous) function

$$\boldsymbol{\phi} \mapsto \boldsymbol{\Phi}(\boldsymbol{\phi})$$

maps vectors from the convex compact set S_M to S_M. Brouwer's fixed point theorem therefore guarantees that there is a solution $\hat{\boldsymbol{\phi}}$ to the equation $\boldsymbol{\phi} = \boldsymbol{\Phi}(\boldsymbol{\phi})$. The frequencies $f_{ij} = \hat{\phi}_j$ $(i = 2, ..., L+1, j = 1, ..., M)$ therefore solve equation (A.1b), provided that $\mathbf{x}$ is known.

We can follow exactly the same procedure with Eq. (A.1a). Let $\boldsymbol{\psi} \in S_M$ a vector of frequencies and let

$$\Psi_k(\boldsymbol{\psi}) = \frac{(1-d_k)\psi_k}{1-d_k+I_1} + d_k q\gamma s \sum_{l=1}^M \frac{\psi_l}{1-d_l+I_1} x_k$$

Once again, $\sum_{k=1}^M \Psi_k(\boldsymbol{\psi}) = \sum_{l=1}^M \psi_l = 1$, and Brouwer's fixed point theorem guarantees a solution $\hat{\boldsymbol{\psi}}$ to the equation $\boldsymbol{\psi} = \boldsymbol{\Psi}(\boldsymbol{\psi})$. The frequencies $f_{1j} = \hat{\psi}_j$ $(j = 1, ..., M)$ therefore solve Eq. (A.1a), provided that $\mathbf{x}$ is known. In the following, we write $\hat{\phi}_j$ as $\hat{\phi}_j(\mathbf{x})$ and $\hat{\psi}_j$ as $\hat{\psi}_j(\mathbf{x})$ to emphasize that they depend on which frequency vector was used to obtain them.

In the second step, define the map $\mathbf{x} \mapsto \mathbf{x}'(\mathbf{x})$ with

$$x'_k = p_1\hat{\psi}_k(\mathbf{x}) + \sum_{i=2}^{L+1} p_i\hat{\phi}_k(\mathbf{x}) = p_1\hat{\psi}_k(\mathbf{x}) + (1-p_1)\hat{\phi}_k(\mathbf{x})$$

As $\hat{\boldsymbol{\psi}}, \hat{\boldsymbol{\phi}} \in S_M$ and $0 \leq p_1 \leq 1$, $\mathbf{x}'$ is a vector in S_M. Since $\mathbf{x} \in S_M$, too, Brouwer's fixed point theorem applies to the map $\mathbf{x} \mapsto \mathbf{x}'(\mathbf{x})$. This guarantees the existence of a solution $\hat{\mathbf{x}}$ such that

$$\hat{x}_k = p_1\hat{\psi}_k(\hat{\mathbf{x}}) + (1-p_1)\hat{\phi}_k(\hat{\mathbf{x}})$$

for all k.

The frequencies $f_{1k} = \hat{\psi}_k(\hat{\mathbf{x}})$, $f_{ik} = \hat{\phi}_k(\hat{\mathbf{x}})$ $(i = 2, ..., L+1, k = 1, ..., M)$ solve the equilibrium equations (A.1a) and (A.1b) and also satisfy $\hat{x}_k = \sum_{i=1}^{L+1} p_i f_{ik}$ for $k = 1, ..., M$. Since $f_{ik} = n_{ik}/p_i$ is the same for all clusters $i = 2, ..., L+1$, this is a symmetric equilibrium.

Note that Brouwer's theorem ensures that a fixed point exists, but does not imply that it is unique. Multiple solutions for $\hat{\boldsymbol{\phi}}$ lead to the asymmetric equilibria described in the main text.

Appendix B

To prove that in monomorphic populations $\bar{d}_0 = 0$ is repelling, we approximate the selection gradient

$$G(d) = \left.\frac{\partial F(d_{mut}, d)}{\partial d_{mut}}\right|_{d_{mut}=d}$$

with its Taylor expansion near $d = 0$,

$$G(d) = G(0) + G'(0) \cdot d + O(d^2) = 0 + dq\gamma s^2[(1-p)(1-q) + q\gamma] + O(d^2)$$

which is positive for sufficiently small d whenever the assumptions $q, \gamma, s > 0$ are satisfied. The positive selection gradient means that mutants with higher dispersal can invade and $\bar{d}_0 = 0$ is always repelling.

Appendix C

In this Appendix, we investigate the roots $\bar{d}_{1,2}$ given in equation (7). First we prove that the roots are real, i.e., that A/B is positive. From its definition in (8), it is obvious that $0 < B \leq 1$ (recall the assumptions $0 < p < 1$, $q, \gamma, s > 0$). To see that A is positive, notice that A is linear in p and therefore its value must be between

$$A|_{p=0} = (1-q)(1-(1-q)s)^2 + q\gamma\left[1-(1-q)s(2-(1-q)s)\right]$$

and

$$A|_{p=1} = q\gamma\left[1+(1-q)s(2+(1-q)s)\right]$$

$A|_{p=1}$ is strictly positive. To see that $A|_{p=0}$ is non-negative, notice that it is linear in γ, and therefore it must be between

$$A|_{p=0,\gamma=0} = (1-q)(1-(1-q)s)^2$$

and

$$\begin{aligned} A|_{p=0,\gamma=1} &= (1-q)(1-(1-q)s)^2 + q\left[1-(1-q)s(2-(1-q)s)\right] \\ &= (1-q)(1-s)^2 + q(1-(1-q)s^2) \end{aligned}$$

which are both non-negative. Hence for all $p > 0$, A must be positive.

Next, we show that

$$\bar{d}_2 = \frac{2}{2 + \left[1 - s(1-q+2q\gamma) - \sqrt{A/B}\right]}$$

is not in the interval $[0, 1)$, i.e., that the bracketed expression in the denominator is non-positive. If $1 - s(1-q+2q\gamma)$ is negative, then this is obviously so. If $1 - s(1-q+2q\gamma)$ is non-negative, then

$$1 - s(1-q+2q\gamma) \leq \sqrt{A/B}$$

is equivalent to

$$A - (1 - s(1 - q + 2q\gamma))^2 B \geq 0$$

After substituting A and B from (8), the left hand side of this inequality can be rearranged into $4q\gamma s(1 - q(1 - \gamma))(1 - sB)$, which is non-negative since $0 < B \leq 1$.

An analogous argument shows that

$$\bar{d}_1 = \frac{2}{2 + \left[1 - s(1 - q + 2q\gamma) + \sqrt{A/B}\right]} \leq 1$$

This inequality holds whenever the bracketed expression in the denominator is non-negative, i.e., if either $1 - s(1 - q + 2q\gamma)$ is non-negative or, if it is negative, $A - (1 - s(1 - q + 2q\gamma))^2 B \geq 0$ holds; the latter has been shown above.

Finally, we show that $\bar{d}_1$ always exceeds $1/2$. Write

$$\bar{d}_1 = \frac{2}{4 - \left[1 + s(1 - q + 2q\gamma) - \sqrt{A/B}\right]}$$

to see that $\bar{d}_1 > 1/2$ holds whenever the bracketed expression is positive (since we already have that $\bar{d}_1 \leq 1$, we know that the denominator does not change sign). The bracketed expression is positive when

$$(1 + s(1 - q + 2q\gamma))^2 B - A > 0$$

After some algebra, the left-hand side of this inequality can be rewritten as

$$4s(1 - q + q\gamma)((1 - p)(1 - q) + q\gamma sB) + 4q\gamma sB$$

which is indeed strictly positive.

Appendix D

Here we consider four limiting cases of our model, each of which recovers the evolutionarily stable dispersal strategy of the Hamilton–May (1977) model.

Assume first that all dispersed offspring enter the global dispersal pool, i.e., $q = 1$. This implies that every dispersed offspring survives dispersal with probability γs. In this case, there is no difference in connectivity, and it is irrelevant whether a site is solitary or is in a cluster. The mutant projection matrix in (6) simplifies to

$$\mathbf{A}_{mut} = \begin{bmatrix} \alpha + \beta p & \beta p \\ \beta(1 - p) & \alpha + \beta(1 - p) \end{bmatrix} = \alpha \mathbf{I} + \beta \mathbf{P}$$

where $\alpha = (1 - d_{mut})/(1 - d_{mut} + \gamma sd)$, $\beta = d_{mut}\gamma s/(1 - d + \gamma sd)$, $\mathbf{I}$ is the identity matrix, and

$$\mathbf{P} = \begin{bmatrix} p & p \\ 1 - p & 1 - p \end{bmatrix}$$

Recall that the eigenvalues of a matrix of the form $\alpha\mathbf{I} + \beta\mathbf{P}$ are $\alpha + \beta\lambda_P$, where λ_P stands for the eigenvalues of $\mathbf{P}$. Since $\mathbf{P}$ is a singular stochastic matrix, its eigenvalues are 1 and 0. The leading eigenvalue of $\mathbf{A}_{mut}$ is therefore

$$\alpha + \beta = \frac{1 - d_{mut}}{1 - d_{mut} + \gamma s d} + \frac{d_{mut}\gamma s}{1 - d + \gamma s d}$$

which is the invasion fitness of a mutant d_{mut} in the resident population d in the Hamilton–May (1977) model with survival probability $\sigma = \gamma s$. Hence the pairwise invasibility plots of the present model with $q = 1$ are the same as those of the of the Hamilton–May model (Figure 7a). In particular, the boundaries between the invasion and non-invasion areas, given by $\lambda_1 = 1$, are two straight lines, the main diagonal $d_{mut} = d$ and $d_{mut} = 1 - (1 - \gamma s)d$, and the evolutionarily stable dispersal strategy is $d^* = 1/(2 - \gamma s)$.

Second, assume that all sites are in the cluster(s), i.e., $p = 0$. The mutant projection matrix in (6) is then a lower triangular matrix. This means that the matrix is reducible, and the invasion fitness cannot be defined unequivocally (invasion may depend on where the mutant appears). However, since the eigenvalues of a matrix depend continuously on the matrix elements, the eigenvalues of this triangular matrix are informative for the limit $p \to 0$ of irreducible ($p > 0$) systems. The eigenvalues of the triangular matrix are its diagonal elements,

$$\lambda_1 = \frac{1 - d_{mut}}{1 - d_{mut} + q\gamma s d}$$

and

$$\lambda_2 = \frac{1 - d_{mut}}{1 - d_{mut} + [q\gamma s + (1 - q)s]d} + \frac{d_{mut}[q\gamma s + (1 - q)s]}{1 - d + [q\gamma s + (1 - q)s]d}$$

The first eigenvalue is always less than 1, so that the mutant can invade if $\lambda_2 > 1$ (note that for sufficiently small d_{mut}, $\lambda_1 > \lambda_2$ is the leading eigenvalue, so that λ_2 is not always the invasion fitness but always a valid fitness proxy). λ_2 is the same as the invasion fitness of the Hamilton–May (1977) model with survival probability $\sigma = [q\gamma s + (1 - q)s]$, the survival probability of offspring who disperse from a cluster. Hence the fitness proxy of this limiting model coincides with the invasion fitness of the corresponding Hamilton–May model, and so do the evolutionary singularity and its stability properties.

Third, assume that all sites are solitary, i.e., $p = 1$. This implies that dispersed offspring survive with probability $q\gamma s$ (recall that if an offspring dispersed from a solitary site does not enter the global dispersal pool, it vanishes). The mutant projection matrix in (6) is now an upper triangular matrix with eigenvalues

$$\lambda_1 = \frac{1 - d_{mut}}{1 - d_{mut} + q\gamma s d} + \frac{d_{mut} q\gamma s}{1 - d + q\gamma s d}$$

and

$$\lambda_2 = \frac{1 - d_{mut}}{1 - d_{mut} + q\gamma s d + (1 - q)s d} + \frac{d_{mut} s(1 - q)}{1 - d + q\gamma s d + (1 - q)s d}$$

and, as above, the eigenvalues of the irreducible system with $p < 1$ go to these eigenvalues as

$p \to 1$. For $d_{mut} = d$, the first eigenvalue is $\lambda_1 = 1$ and the second eigenvalue is less than 1. By continuity, also for small mutations ($d_{mut} = d \pm \epsilon$) λ_1 is the leading eigenvalue of the mutant projection matrix, and λ_1 is again the invasion fitness in the Hamilton–May (1977) model with survival probability $\sigma = q\gamma s$. This proves that in the neighbourhood of $d_{mut} = d$, invasion/noninvasion coincides with invasion/noninvasion in the Hamilton–May model. Therefore the evolutionary singularities and their stability properties also coincide with those of the corresponding Hamilton–May model, i.e., there is a unique singular strategy which is both convergence stable and evolutionarily stable.

However, the pairwise invasibility plot of the present model with $p \to 1$ differs from that of the Hamilton–May (1977) model outside the neighbourhood of the main diagonal $d_{mut} = d$, and the present model exhibits coexistence of different dispersal strategies, which is impossible in the Hamilton–May model (see Figure 7b for an example). The reason for this discrepancy is that even with $p \to 1$, the model assumes infinitely many well-connected sites in the clusters; only the fraction of these sites goes to zero. A dispersal strategy adapted to well-connected sites can coexist with the one adapted to the solitary sites even though it will be constrained to the clusters are therefore will attain only an infinitesimal relative frequency in the population (see Kisdi 2016 for a more detailed discussion).

Fourth, assume that $q\gamma = 0$, i.e., no offspring enters the global dispersal pool ($q = 0$) or no one in the global dispersal pool survives ($\gamma = 0$). In both of these cases, the solitary sites are isolated and the mutant projection matrix in (6) simplifies to a diagonal matrix. The eigenvalues of the mutant projection matrix are 1 and

$$\lambda_{HM}(d_{mut}, d) = \frac{1 - d_{mut}}{1 - d_{mut} + (1-q)sd} + \frac{d_{mut}(1-q)s}{1 - d + (1-q)sd}$$

which is the invasion fitness in the Hamilton–May (1977) model with survival probability $\sigma = (1-q)s$ (a dispersed offspring may survive only if it remains in the local dispersal pool; this further simplifies to s in case $q = 0$). Since the diagonal matrix is reducible, we need to assume $q\gamma > 0$ and consider the limit $q\gamma \to 0$; and because 1 is an eigenvalue with $q\gamma = 0$, we need to make a formal expansion of the mutant projection matrix and of the invasion fitness proxy in terms of $q\gamma$. This results in the first order approximation

$$F(d_{mut}, d) = 1 + g(d_{mut}, d)\,[1 - \lambda_{HM}(d_{mut}, d)]\,q\gamma + O((q\gamma)^2)$$

with

$$g(d_{mut}, d) = \frac{d_{mut} ps}{1 - d} - \frac{ds}{1 - d_{mut}}$$

For any fixed $q\gamma > 0$, the trace of the mutant projection matrix is less than 2 when d_{mut} is sufficiently close to d, and therefore the fitness proxy F can be used in the neighbourhood of $d_{mut} = d$ (Metz and Leimar 2011). Since $g(d, d) = -(1-p)ds/(1-d) < 0$, by continuity $g(d_{mut}, d)$ is negative for d_{mut} sufficiently close to d. In the neighbourhood of $d_{mut} = d$, therefore, $F(d_{mut}, d) \gtreqless 1 \Leftrightarrow \lambda_{HM}(d_{mut}, d) \gtreqless 1$, so that the evolutionary singularities and their stability properties coincide with those of the Hamilton–May model. As with $p \to 1$, however, the pairwise invasibility plot differs from that of the Hamilton–May model and coexistence is possible away from the diagonal.

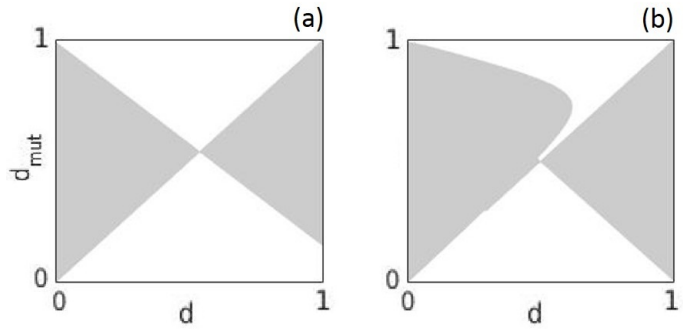

Figure 7: Pairwise invasibility plots for $s = 0.8$, $\gamma = 0.2$ and (a) $q = 1$, $p = 0.9$ and (b) $q = 0.1$, $p \to 1$. Shaded areas: the mutant can invade; white: the mutant dies out. Coexistence by mutual invasibility occurs where the shaded area overlaps with its mirror image on the diagonal $d_{mut} = d$ (Geritz et al. 1998).